# AIAA 2004–4325

# Multiobjective Optimization Using Approximation Model-Based Genetic Algorithms

Hyoung-Seog Chung
*Republic of Korea Air Force Academy*

and
Juan J. Alonso
*Stanford University, Stanford, CA 94305*

# 10th AIAA/ISSMO Symposium on Multidisciplinary Analysis and Optimization
## August 30–September 1 , 2004/Albany, New York

# Multiobjective Optimization Using Approximation Model-Based Genetic Algorithms

Hyoung-Seog Chung[*]
*Republic of Korea Air Force Academy*

and

Juan J. Alonso[†]
*Stanford University, Stanford, CA 94305*

**Realistic high-dimensional MDO problems are more likely to have multimodal search spaces and they are also mutiobjective in nature. Genetic Alogrithms(GAs) are becoming popular choices for better global and multiobjective optimization frameworks to fully realize the full benefits of conducting MDO. One of the biggest drawbacks of GAs, however, is that they require many function evaluations to achieve a reasonable improvement within the design space. Therefore, the efficiency of GAs has to be improved in some way before they can be truly used in high-fidelity MDO. In this work, a multiobjective design optimization framework is developed by combining GAs and an approximation technique called Kriging method which can produce fairly accurate global approximations to the actual design space to provide the function evaluations efficiently. It is applied to a low boom supersonic business jet design problem and its results demonstrate the efficiency and applicability of the proposed design framework. Furthermore, the possibility of using the Kriging approximation models as computationally inexpensive gradient estimators to accelerate the GA process is investigated.**

## 1. Introduction

THE conceptual and preliminary phases of the design of aerospace systems involve searching for either improved or optimal combinations of design variables within large design spaces. In this process, a number of trades between the performance of various different disciplines is considered before arriving at a solution. Because of the nonlinearities and complex interactions among the design variables and disciplines, realistic high-dimensional multidisciplinary design optimization(MDO) problems are more likely to have multimodal search spaces than single discipline design problems. In addition, some of the design variables in real-life engineering problems could be discrete in nature, and it is always possible to encounter a non-differentiable or discontinuous region of the design space. Therefore, traditional gradient-based optimization methods which use first and/or second derivatives of the objective function to arrive at an optimum will not necessarily provide the necessary robustness required for MDO problems, particularly with respect to the ability to handle a wide range of problems.

Typical MDO problems are also multiobjective in nature. Unlike single-objective optimization where optimality with respect to a single scalar function is pursued, multiobjective optimization may result in a set of optimal solutions which represent the trade-off surface between the conflicting criteria. These non-dominated solution points are called Pareto optimal solutions. None of the solutions in the Pareto optimal set is absolutely better than any other with respect to all the objectives in question; therefore, any one of them is an acceptable solution and can be considered "optimum" in some respect. Once the set of optimal solutions is identified, the designer has the freedom of choosing one solution out of many possible alternatives based on experience, prior knowledge and other criteria or constraints particular to the current design problem. One way to simplify the multiobjective optimization problem is to create a linear combination of the objectives. Then the process becomes a single-objective optimization, but it also includes the difficulty of choosing right values for weighting factors for each objective function contribution. The outcome of this simplified process will largely depend on the vector of weights used in the linear combination. These shortcomings of traditional optimization methods result in the need for better global and multiobjective optimization frameworks to fully realize the full benefits of conducting MDO.

Genetic Algorithms (GAs) are search and optimization methods based on mechanics of natural selection and adaptation. Pioneered by John Holland, they

---

AMERICAN INSTITUTE OF AERONAUTICS AND ASTRONAUTICS PAPER 2004–4325

have recently been gaining much attention as a popular choice for various real-world engineering problems largely due to their robustness and simplicity. GAs have many advantages that make them suitable for MDO. Because they operate with a population of possible solutions rather than a single candidate, they are less likely to get stuck in a false local minima. Furthermore, a number of Pareto optimal solutions may be captured during one run of GA. They are relatively simple and easy to use and don't require any auxiliary information such as gradients other than the evaluation of the (possibly) multiple objective functions. This simplicity allows users to integrate them to existing software or computational modules without significant modification. In addition, they can take advantage of rapidly growing parallel computing power more easily. These merits make GAs very appealing as more reasonable candidate optimization tools for MDO.[1]

One of the biggest drawbacks of GAs, however, is that they require hundreds, if not thousands, of function evaluations to achieve a reasonable improvement within the design space. This is particularly due to the slow random search procedure used which is only directed by one criterion of fitness level. Thus, the robustness of the method comes with the price of low computational efficiency. Even though some researchers have recently demonstrated their promise in certain classes of realistic design problems, their use is often infeasible for high-fidelity models since the cost of carrying out the necessary function evaluations can be exorbitantly high.

The efficiency of GAs has to be improved in some way before they can be truly used in high-fidelity MDO. Given prior work with computationally inexpensive and efficient approximation techniques such as the Kriging and Cokriging methods, which can produce fairly accurate global approximations to the actual design space, the combination of GAs with these approximation models becomes an obvious approach to overcome the problems of GAs mentioned above. Since the computational cost to estimate the objective function once the approximation model is constructed is fairly low, the slow convergence rate and the large computational burden to obtain many function evaluations for GA methods are not significant any more. If the approximation model is accurate enough, it can even provide auxiliary information such as gradients to accelerate the GA process even further. Moreover, the approximation models can also be used to enhance the performance of each genetic operators such as crossover and mutation as well as to guide the population initialization. The initialization, crossover and mutation are usually carried out randomly. Thus, these operations guided by an approximate model even with lower accuracy should usually better than do them randomly. [2] The approximation model itself can be benefited from the rich data base accumulated from GA run. Their accuracy can be sequentially improved by updating the sample data set with the function evaluation performed by high-fidelity code during the GA runs or the validation phase. The potential mutual benefits of combining these two methods can provide an efficient and robust design framework necessary in MDO.

## 2. Overview of Kriging Method

The Kriging technique uses a two component model that can be expressed mathematically as

$$y(\boldsymbol{x}) = f(\boldsymbol{x}) + Z(\boldsymbol{x}), \tag{1}$$

where $f(\boldsymbol{x})$ represents a global model and $Z(\boldsymbol{x})$ is the realization of a stationary Gaussian random function that creates a localized deviation from the global model.[6] $f(x)$ can be considered to be an underlying constant, $\beta$,[5] and then equation (1) becomes

$$y(\boldsymbol{x}) = \beta + Z(\boldsymbol{x}), \tag{2}$$

which is used in this paper. The estimated model of equation (2) is given as

$$\hat{y} = \hat{\beta} + \boldsymbol{r^T}(\boldsymbol{x})\boldsymbol{R^{-1}}(\boldsymbol{y} - \boldsymbol{f}\hat{\beta}), \tag{3}$$

where $\mathbf{y}$ is the column vector of response data and $f$ is a column vector of length $n_s$ which is filled with ones. $\mathbf{R}$ in equation (3) is the correlation matrix which can be obtained by computing $R(x^i, x^j)$, the correlation function between any two sampled data points. This correlation function is specified by the user. In this work, the authors use a Gaussian exponential correlation function of the form provided by Giunta, et al.[3]

$$R(\boldsymbol{x^i}, \boldsymbol{x^j}) = \exp[-\sum_{k=1}^{n} \boldsymbol{\theta_k} |\boldsymbol{x_k^i} - \boldsymbol{x_k^j}|^2]. \tag{4}$$

The correlation vector between $x$ and the sampled data points is expressed as

$$\boldsymbol{r^T}(\boldsymbol{x}) = [\boldsymbol{R(x, x^1)}, \boldsymbol{R(x, x^2)}, ..., \boldsymbol{R(x, x^n)}]^{\boldsymbol{T}}. \tag{5}$$

The value for $\hat{\beta}$ is estimated using the generalized least squares method as

$$\hat{\beta} = (\boldsymbol{f^T R^{-1} f})^{-1} \boldsymbol{f^T R^{-1} y}. \tag{6}$$

Since $R$ is a function of the unknown variable $\theta$, $\hat{\beta}$ is also a function of $\theta$. Once $\theta$ is obtained, equation (3) is completely defined. The value of $\theta$ is obtained by maximizing the following function over the interval $\theta > \mathbf{0}$

$$-\frac{[n_s \ln(\hat{\sigma}^2) + \ln |\boldsymbol{R}|]}{2}, \tag{7}$$

where

$$\hat{\sigma}^2 = \frac{(\boldsymbol{y} - \boldsymbol{f}\hat{\beta})^T \boldsymbol{R^{-1}}(\boldsymbol{y} - \boldsymbol{f}\hat{\beta})}{n_s}. \tag{8}$$

This requires the solution of a k-dimensional unconstrained non-linear optimization problem, which can be reduced to a one-dimensional problem by assuming the same correlation parameter for each component of the sample points. Thus, equation (4) can be simplified as

$$R(\boldsymbol{x^i}, \boldsymbol{x^j}) = \exp[-\theta \sum_{k=1}^{n} |\boldsymbol{x_k^i} - \boldsymbol{x_k^j}|^2]. \qquad (9)$$

## 3. Advanced Genetic Algorithms

### 3.1 Multiobjective Genetic Algorithms

Many real-world optimization problems, especially in MDO situations, require the process of simultaneous optimization of possibly conflicting multiple objectives, and this is termed multiobjective optimization. By definition, the multiobjective optimization has a very different nature from that of single-objective optimization. Unlike single-objective optimization where only one optimal solution is pursued, a typical multiobjective optimization problem produces a set of solutions which are superior to the rest of the solutions with respect to all objective criteria but are inferior to other solutions in one or more objectives. These solutions are known as Pareto optimal solutions or nondominated solutions. None of the solutions in the Pareto optimal set is absolutely better than any others with respect to all the objectives concerned; therefore, any one of them is an acceptable solution. Once the set of optimal solutions is identified, the designers have the freedom of choosing one solution out of many possible solutions based on their experience and prior knowledge and other criteria or constraints.

A genetic algorithm can use the above defined dominance criteria in a straightforward fashion, to drive the search process toward the Pareto front. Due to the unique feature of GAs, which work with a population of solutions, multiple Pareto optimal solutions can be captured in a single simulation run. This is the primary reason that makes GAs highly suitable to be used in multiobjective optimization.

A recent study by Coello[8] proposed a micro-GA based multiobjective optimization utilizing an external file to store nondominated vectors found in previous generations to accelerate the multiobjective optimization procedure. The method implemented additional elitism strategy and adaptive grid-type technique to accelerate the convergence and to keep the diversity in Pareto front. Micro-GAs is a specialized GA that works with a very small population size of usually 3-6 and a reinitialization process. The previous studies[8,9] showed that micro-GAs achieved a faster convergence rate than simple GAs. In the present research, some of the ideas of Coello's work were adopted to a single objective micro-GA along with the traditional Goldberg's Pareto ranking approach in order to develop an efficient and robust design framework. The authors
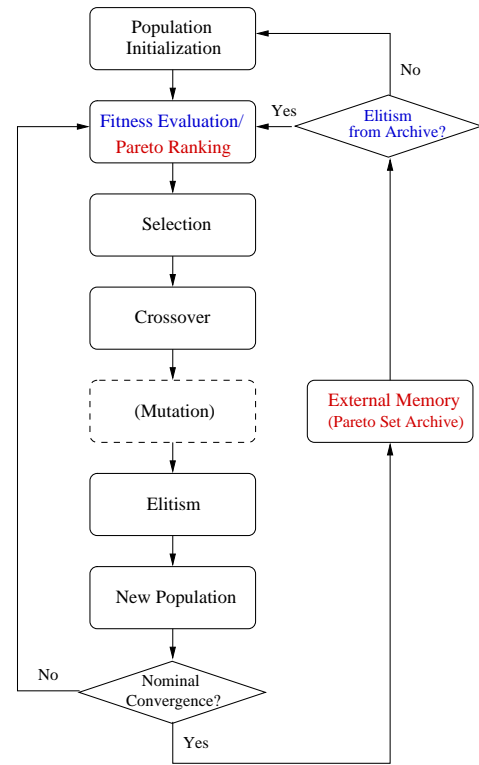


**Fig. 1    Flow Chart for Multiobjective GA**

modified a micro-GA originally developed by Carroll[10] from CU Aerospace for that purpose.

The procedure is illustrated in Figure 1. First, a random population is generated and their objective values are calculated just like in the original micro-GA. Then, to ensure all the nondominated individuals to have same level of reproductive potential, Goldberg's nondominated sorting procedure is implemented. Therefore, the fitness level of each individual is determined based on the nondomination criterion rather than the objective function value itself.

Based on the rank of nondominance, the population goes through the usual operators of micro-GA, namely selection and crossover and check if the nominal convergence among the population points is reached. If not converged, it returns to the function evaluation and nondominance ranking steps for the new generation, otherwise it goes to the reinitialization step.

Two types of elitism are implemented in the reinitialization step. The first type is to pass the best solutions from the previous nominal convergence stage. This is the same elitism strategy as in the single objective micro-GA. The second type involves the storing of nondominated vectors produced from each cycle of micro-GA to a external file and inserting some of the best solutions generated so far as the reinitialized population for the micro-GA. This process is applied at certain intervals for the intention of improving the nondominated solutions by getting closer to the true Pareto front or by getting a better distribution.

### 3.3 Approximation Model based micro-GA

Once fairly accurate global approximation models are constructed with computationally efficient techniques such as the Kriging or Cokriging methods, combining them with GAs becomes an obvious choice to overcome the computational burden presented by GAs. Since the computational cost of estimating the objective function through the approximation models is trivial, the slow convergence rate of GAs leading to many generations and function evaluations to get to the optimal solution would not matter any more. If the approximation model is accurate enough, it can even provide auxiliary information such as gradients to accelerate the process even further. In addition, GAs are more suitable approaches than gradient-based methods for use with approximation models that can support multmodal functions.

The approximation model itself can benefit from the use of a direct GA by recycling the rich dataset produced by each population. The mutual benefits of combining these two methods can provide the efficient and robust design framework necessary in MDO. Another way of using approximation models for accelerating the GA process is to use them as a gradient estimators to provide the necessary gradient information for the hybrid micro-GA proposed in the previous section. Even though adjoint method can provide gradient information cheaply and efficiently, the derivation of the adjoint equations and boundary conditions can not be carried out for arbitrary cost functions. In addition, an adjoint code implementation might take months of validation. Therefore, the approximation models can be a useful and inexpensive alternative for computing the gradients.

## 4. Design Problem : Low-Boom Supersonic Business Jet (SBJ) Design

The design problem in question involves the ground boom and drag minimization of a supersonic business jet wing-body-tail configuration at a specified lift coefficient, $C_L = 0.1$, which corresponds to a cruise weight of $100,000$ lbs at a cruise flight altitude of $50,000$ ft with reference area of $1,032 \ ft^2$. The free-stream flow conditions were fixed at $M_\infty = 1.5$. The aircraft geometry and flow conditions were parameterized directly in CAD using 108 potential design variables.[11] The list of geometric design variables for 15-dimensional design problem is given in Table 1.

The wing planform for this configuration was designed with experience from the NASA HSR program to have a portion with a subsonic leading edge followed by an outboard panel with a supersonic leading edge to aid in increasing the span to achieve better low-speed performance. The airfoil sections for the outboard portion of the main wing and the horizontal tail were chosen to be simple biconvex airfoils of

varying thickness, while an RAE2822 was used for the inboard part of the main wing with a subsonic leading edge. Fuselage aft-mounted nacelles are included in the baseline design, although their presence was not modeled in this optimization.

A CFD/boom analysis of the two objective criteria considered in this study: ground boom initial overpressure and $C_D$, yield values for the baseline design of $C_D = 0.009189$ and $\Delta p = 0.7898 \text{psf}$ respectively. All improvements in either or both of these criteria are measured against the value for this baseline configuration.

The values of vertical displacement defined at six different locations were transferred to the fuselage radii distribution at 15 different stations along the body through spline interpolation. In this way, the number of design variables used to define the overall fuselage shape could be minimized. The initial values of the design variables are presented in Table 2. The design space was limited by imposing upper and lower bounds on each design variable. Some of the bounds were chosen such that the regeneration of meshes used in the QSP107 calculation would not fail, and thus ensuring the automation of the entire procedure. The limits are also listed in Table 1.

## 5. Design Tools

In order to develop Kriging approximation models, a large number of CFD computations for different geometries must be carried out automatically. For this purpose, we have developed a nonlinear integrated boom analysis tool, QSP107, that can provide both ground boom and aerodynamic performance information for a small set of configuration variables that are provided in an input file.

### 5.1 QSP107

QSP107 is a nonlinear integrated tool for both sonic boom prediction and aerodynamic performance analysis based on fully nonlinear CFD. This tool couples the multiblock Euler and Navier-Stokes flow solver for structured mesh, FLO107-MB,[13] to a CAD-based geometry kernel and a mesh perturbation procedure for efficient mesh regeneration, and to the PC Boom software for far-field propagation developed by Wyle Associates.[14] A flowchart of the automated analysis process can be seen in Figure 2.

The procedure starts with a CAD-based geometry generation module called Aerosurf that automatically generates the necessary surface meshes to describe the configuration in question. This geometry module is based on a parametric aircraft description with 108 design variables of which a subset (either two or fifteen) are chosen for our optimization applications. Aerosurf is a parallel geometry generation module that uses parametric CAD modeling concepts to allow for the parameterization of the shape of complete aircraft.

Aerosurf relies on the CAPRI CAD interface of Haimes [11, 12] to provide access to a number of parametric CAD softwares including Pro/Engineer, CATIA V5, Solid-Works, and I-DEAS. Parametric aircraft models of arbitrary complexity can be created and used within this environment, thus automating some of the most complicated geometry manipulations that are the heart of any high-fidelity design procedure.

An initial multiblock mesh is generated using the Gridgen software[15] for the baseline design configuration and then it is passed to a mesh perturbation routine called Meshwarp that can handle arbitrary configurations and generate volume meshes corresponding different surface geometries. As constructed, the meshes have higher resolution in the areas where shock waves and expansions are present below the aircraft, and the grid lines are slanted at the Mach angle to maximize the resolution of the pressure signature at distance of the order of one fuselage length below the aircraft. The user may specify the location of an arbitrary cylindrical surface where the near-field signature is extracted from the multiblock flow solution and then provided as an input to a modified version of PC Boom which propagates a full three-dimensional signature along all rays that reach the ground. This allows for the calculation of arbitrary cost functions (not only ground-track initial overpressure) that may involve weighted integration of the complete sonic boom footprint. In this work, however, only the ground track overpressure have been considered.

The flow solver, FLO107-MB, combines advanced multigrid procedures and a preconditioned explicit multistage time-stepping algorithm which allows full parallelization. Because of the advanced solution algorithms and parallelization, the integrated tool provides fully nonlinear simulations with very rapid turnaround time. Using typical meshes with over $3 \times 10^6$ mesh points we can obtain a complete flow solution and ground signature in around 7 minutes, using 16 processors of a Beowulf cluster made up of AMD AthlonXP 2100 processors. In this work, QSP107 has been used repeatedly to generate Kriging and Cokriging approximation models and it has also been directly coupled with a genetic algorithm for the design optimization process.

## 6. Results

Two design cycles of the Kriging-based MOGA were performed. Using a latin hypercube sampling(LHS) technique,[16–18] 150 sample points around the baseline design were selected and the values of their design objectives were assigned by QSP107 calculations. The sample data points are plotted as green asterisks and the baseline design point is shown as a pink star in Figure 3 (a). A Kriging model was then generated based on the sample data and used for both function evaluations in the MOGA search.

The estimated components of the Pareto set from the Kriging-based MOGA search procedure are plotted as black circles whereas the CFD validation results of the Pareto set are shown as red asterisks in the figure. The $C_D$ values of the estimated Pareto set from the Kriging-based MOGA and their CFD validation calculations were surprisingly well matched while some of the values of the boom estimations had discrepancies with their CFD counterparts. We can infer that the shape of $C_D$ response is much better behaved having smoothly varying characteristics than that of boom overpressure. Since Kriging assumes a Gaussian distribution for the correlation function between the samples, the accuracy of the Kriging model for $C_D$ is expected to be much higher. On the other hand, the results demonstrate the fact that the boom design space may have a region of discontinuities that cause difficulties in generating accurate Kriging models. However, the estimation produced good design candidates which were all better than the 150 sample points.

The second design iteration was conducted by collecting another 150 sample data points around one of the best design candidates identified during the first design cycle. The Kriging-based MOGA procedure was then repeated. The results are shown in Figure 3 (b). The second sample set is clustered toward the Pareto front as expected, and the estimated Pareto front from the Kriging-based MOGA is amazingly well matched with their CFD validation results. One of the reasons for this outcome is that the confidence level for the Kriging models got higher as the trust region deceased for the second iteration.

With only 300 function evaluations, a very promising Pareto front could be obtained. Again, this result clearly demonstrated the benefits of the Kriging-based MOGA over the original MOGAs directly connected to the CFD function evaluations.

Two of the Pareto solutions found after the second iteration are listed in Table 2: the one for the best $C_D$ case and the one for the best boom case. The best $C_D$ design achieved 15.76% of improvement in $L/D$ over the baseline, while the best boom case achieved a 6.62% improvement. It was found that the biggest contributing factors for the drag reduction were the increase in sweep angle and leading edge extension. LEX is helpful in minimizing drag since it spreads the lift in the streamwise direction, thus decreasing the lift-induced wave drag. It should be noted that the best boom also has a configuration with high sweep angle and large leading edge extension. In fact, these design variables were pushed toward the limits as shown in the table. The author concluded that the increase in sweep angle and leading edge extension was beneficial for both objective criteria; therefore, another constraint should be imposed in future research to prevent the wing geometries from having too high val-

ues of the sweep angle. The aspect ratio for the best $C_D$ design decreased whereas that for the best boom design increased. The wing twist distribution also resulted in additional washout for both cases.

Figures 4 through 7 show the configurations for the best drag and boom designs as well as the corresponding near-field pressure distributions and ground boom overpressures. The best boom design has a fuselage shape having three big expansion regions at the lower side of the body. These expansion regions were achieved by the bump-like shape as shown in Figure 6. These expansion regions caused the breaking down of the shocks coming from the fuselage nose and the wing into smaller shocks, thus producing a much better ground boom criteria as shown in Figure 7. Meanwhile, the fuselage shape of the best drag design was only slightly different from the baseline configuration (Figure 4) compared with the best boom design, especially in the nose region. This result can also be seen in Figure 5 in which the near-field pressure distribution from the forward part of the aircraft has a relatively small difference between the baseline design and the best drag case. This also indicates that the expansion region generated by the wavy shape of the fuselage can play a key role for minimizing boom criteria.

Figures 8, 9 show the configuration and the corresponding ground boom shape for one of the best multiobjective designs from the Pareto solutions. Interestingly, the results are almost identical to the best boom case.

Figure 10 shows the comparison of the flow fields around the aircraft flying at the flight conditions specified. As can be seen, the shock strength coming from the nose and the wing leading edge is greatly reduced to smaller shocks. In addition the strong shock pattern generated from the wing trailing edge area in the baseline configuration is almost eliminated in the optimized configuration.

In conclusion, these figures prove that the proposed procedure constitutes an efficient and robust methodology to be applied to the problems in question. With more design variables and their careful selection, the design process, in the authors' opinion, can produce a better design for low-boom supersonic jets.

# References

[1] Kalyanmoy Deb "An Introduction to Genetic Algorithms," *SADHANA*, Kanpur Genetic Algorithms Laboratory, Kanpur, India, 1999.

[2] Yaochu Jin "A Comprehensive Survey of Fitness Approximation in Evolutionary Computation" *Soft Computing Journal*, 2003

[3] Anthony A. Giunta and Layne T. Watson "A Comparison of Approximation Modeling Techniques: Polynomial Versus Interpolating Models," *7th AIAA/USAF/NASA/ISSMO Symposium on Multidisciplinary Analysis and Optimization* , St. Louis, Missouri, AIAA 98-4758, September 1998.

[4] J. Sacks, W. J. Welch, T. J. Michell, and H. P. Wynn "Design and Analysis of Computer Experiments," *Statistical Science Vol 4. No.4*, pp. 409-453, 1989

[5] Timothy W. Simpson, Timothy M. Mauery, John J. Korte and Farrokh Mistree "Comparison of Response Surface and Kriging Models in the Multidisciplinary Design of an Aerospike Nozzle," *7th AIAA/USAF/NASA/ISSMO Symposium on Multidisciplinary Analysis and Optimization*, St. Louis, Missouri, AIAA 98-4755, September 1998

[6] J. R. Koehler and A. B. Owen "Computer Experiments," *Handbook of Statistics Vol. 13*, pp. 261-308, Elsevier Science, New York, eds. S. Ghosh and C. R. Rao

[7] Edward H. Isaaks and R. Mohan Srivastava *An Introduction to Applied Geostatistics*, Oxford Univ. Press, Oxford, 1989.

[8] C. A. Coello Coello and G. T. Pulido "A Micro-Genetic Algorithms for Multiobjective Optimization," *Proceedings of the Genetic and Evolutionary Computation Conference (GECCO'2001)* , 2001.

[9] K. Krishnakumar "Micro-genetic algorithms for stationary and non-stationary function optimization," *SPIE Proceedings : Intelligent Control and Adaptive Systems, pages 289-296*, 1989.

[10] D. L. Carroll "Fortran Genetic Algorithm Driver," *http://cuaerospace.com/carroll/ga.html*, 2001

[11] J. Alonso, J. Martins and J. Reuther "High-Fidelity Aero-Structural Design of Complete Aircraft Configurations with Aeroelastic Constraints," *21st Applied Aerodynamics Conference*, AIAA 2003-3429, Orlando, FL., 2003.

[12] Hamies, R. and Follen, G. "Computational Analysis Programming Interface," *Proceedings of the 6th International Conference on Numerical Grid Generation in Computational Field Simulations*, Greenwich, 1998

[13] J. J. Reuther, J. J. Alonso, J. C. Vassberg, A. Jameson and L. Martinelli. An Efficient Multiblock Method for Aerodynamic Analysis and Design on Distributed Memory Systems. *AIAA Paper 97-1893*, AIAA Fluid Dynamics Conference. Snowmass, CO. June 1997.

[14] Kenneth J. Plotkin "PCBoom3 Sonic Boom Prediction Model-Version 1.0e," *Wyle Research Report WR 95-22E*, October. 1998.

[15] *Gridgen User Manual ver.13*, Pointwise, Inc., Bedford, 1998

[16] M.D. McKay, R.J. Beckman, and W.J. Conover "A comparison of three methods for selecting values of input variables in the analysis of output from a computer code," *Technometrics*, 21(2):239-245, 1979.

[17] M.L. Stein "Large sample properties of simulations using latin hypercube sampling," *Technometrics*, 29(2):143-151, 1987.

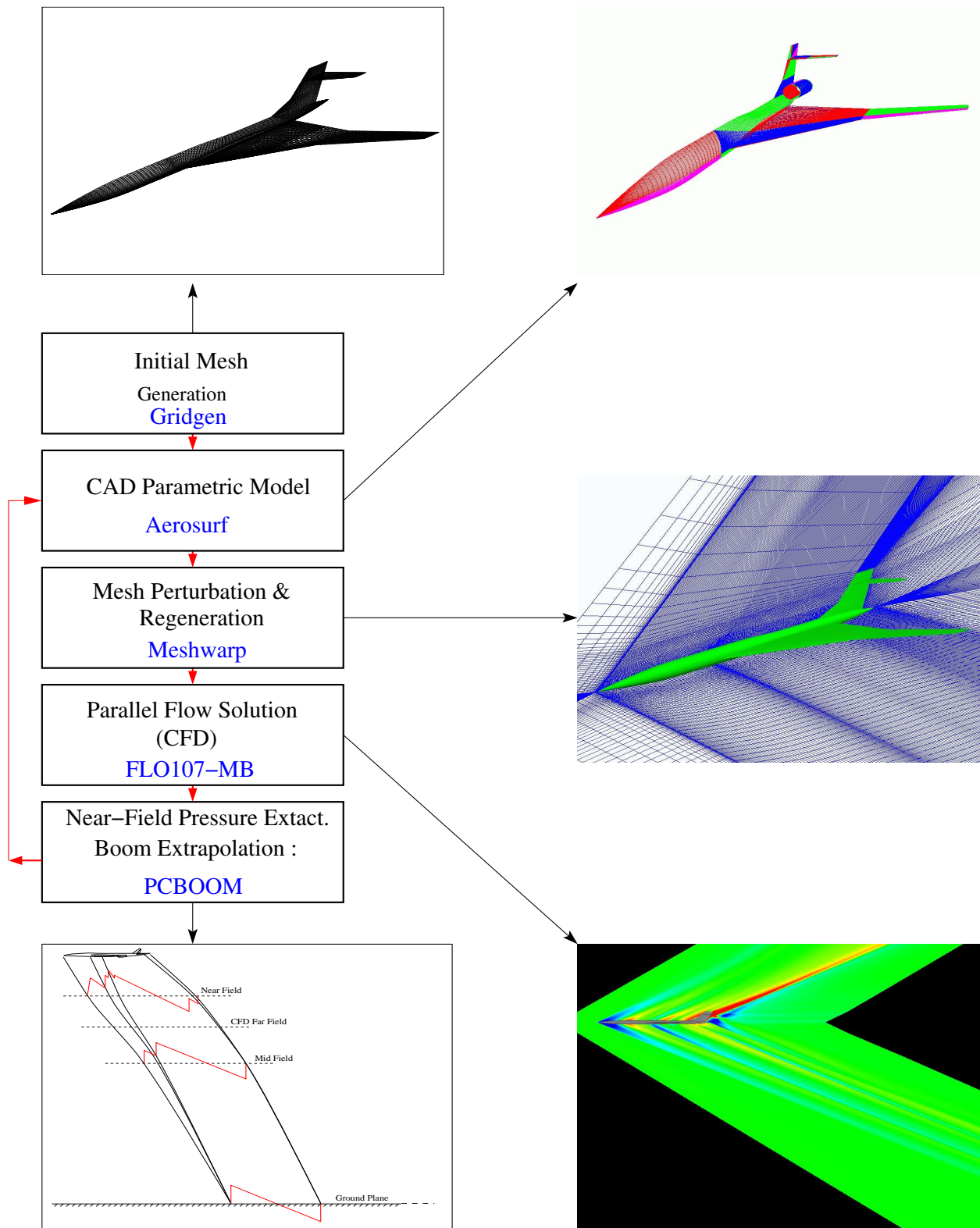[18] *DAKOTA Users Manual Version 3.1*, Sandia National Laboratories, SAND2001-3796, 2003.

American Institute of Aeronautics and Astronautics Paper 2004–4325

**Table 1  Definition of Design Variables and Their Bounds**

| Symbols | Definition | Lower Bounds | Upper Bounds |
|---|---|---|---|
| $x_1$ | wing position along fuselage | 45.0 ft | 65.0 ft |
| $x_2$ | wing dihedral angle | 0.0 deg | 4.0 deg |
| $x_3$ | wing sweep angle | 32.0 deg | 50.0 deg |
| $x_1$ | wing aspect ratio | 4.0 | 7.0 |
| $x_5$ | wing leading edge extension * | 0.75 | 1.25 |
| $x_6$ | wing trailing edge extension * | 0.30 | 0.70 |
| $x_7$ | wing twist angle at root | -1.00 deg | 1.0 deg |
| $x_8$ | wing twist angle at crank | -1.30 deg | 1.3 deg |
| $x_9$ | wing twist angle at tip | -1.50 deg | 1.5 deg |
| $x_{10}$ | vertical displacement of body center at 5% of fuselage length | -0.25 ft | 0.25 ft |
| $x_{11}$ | vertical displacement of body center at 10% of fuselage length | -0.55 ft | 0.55 ft |
| $x_{12}$ | vertical displacement of body center at 20% of fuselage length | -0.80 ft | 0.80 ft |
| $x_{13}$ | vertical displacement of body center at 35% of fuselage length | -0.80 ft | 0.80 ft |
| $x_{14}$ | vertical displacement of body center at 55% of fuselage length | -0.80 ft | 0.80 ft |
| $x_{15}$ | vertical displacement of body center at at 85% of fuselage length | -0.80 ft | 0.80 ft |

**Table 2  15-D Design Optimization Results**

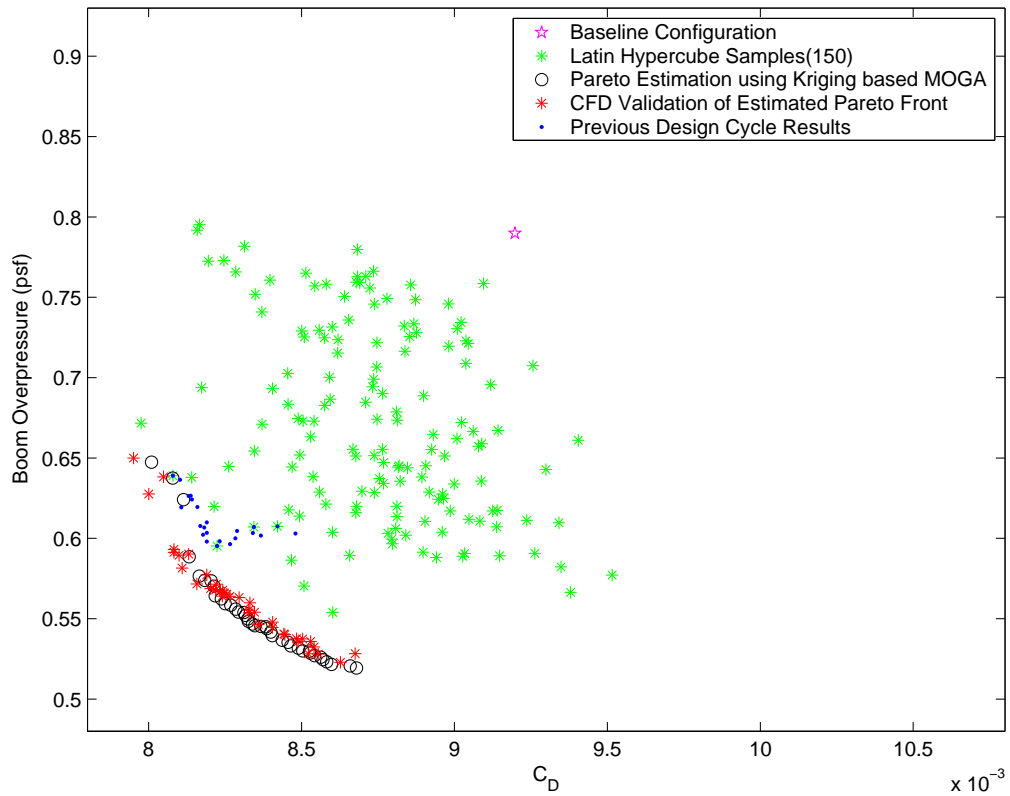| | Baseline Conf. | Best $C_D$ Design | Best Boom Design |
|---|---|---|---|
| (Optimum) Design Variables | $x_1 = 55.00$<br>$x_2 = 1.00$<br>$x_3 = 35.00$<br>$x_4 = 6.00$<br>$x_5 = 1.00$<br>$x_6 = 0.50$<br>$x_7 = 0.00$<br>$x_8 = 0.00$<br>$x_9 = 0.00$<br>$x_{10} = 0.00$<br>$x_{11} = 0.00$<br>$x_{12} = 0.00$<br>$x_{13} = 0.00$<br>$x_{14} = 0.00$<br>$x_{15} = 0.00$ | $x_1 = 54.6901$<br>$x_2 = 0.1025$<br>$x_3 = 49.7494$<br>$x_4 = 5.4848$<br>$x_5 = 1.2410$<br>$x_6 = 0.2286$<br>$x_7 = 0.9952$<br>$x_8 = -0.4004$<br>$x_9 = -0.9216$<br>$x_{10} = 0.0043$<br>$x_{11} = -0.3025$<br>$x_{12} = 0.2091$<br>$x_{13} = 0.3196$<br>$x_{14} = 0.6626$<br>$x_{15} = -0.6369$ | $x_1 = 54.9440$<br>$x_2 = 0.0019$<br>$x_3 = 49.9579$<br>$x_4 = 6.4999$<br>$x_5 = 1.2464$<br>$x_6 = 0.2530$<br>$x_7 = 0.9983$<br>$x_8 = 1.1548$<br>$x_9 = -0.1365$<br>$x_{10} = -0.0231$<br>$x_{11} = -0.3395$<br>$x_{12} = 0.6374$<br>$x_{13} = 0.1330$<br>$x_{14} = 0.7643$<br>$x_{15} = -0.6985$ |
| $C_D$ Results | 0.009198 | 0.007951 | 0.008627 |
| Boom Results | 0.7898 | 0.6450 | 0.5228 |
| $L/D$ | 10.87 | 12.58 | 11.59 |

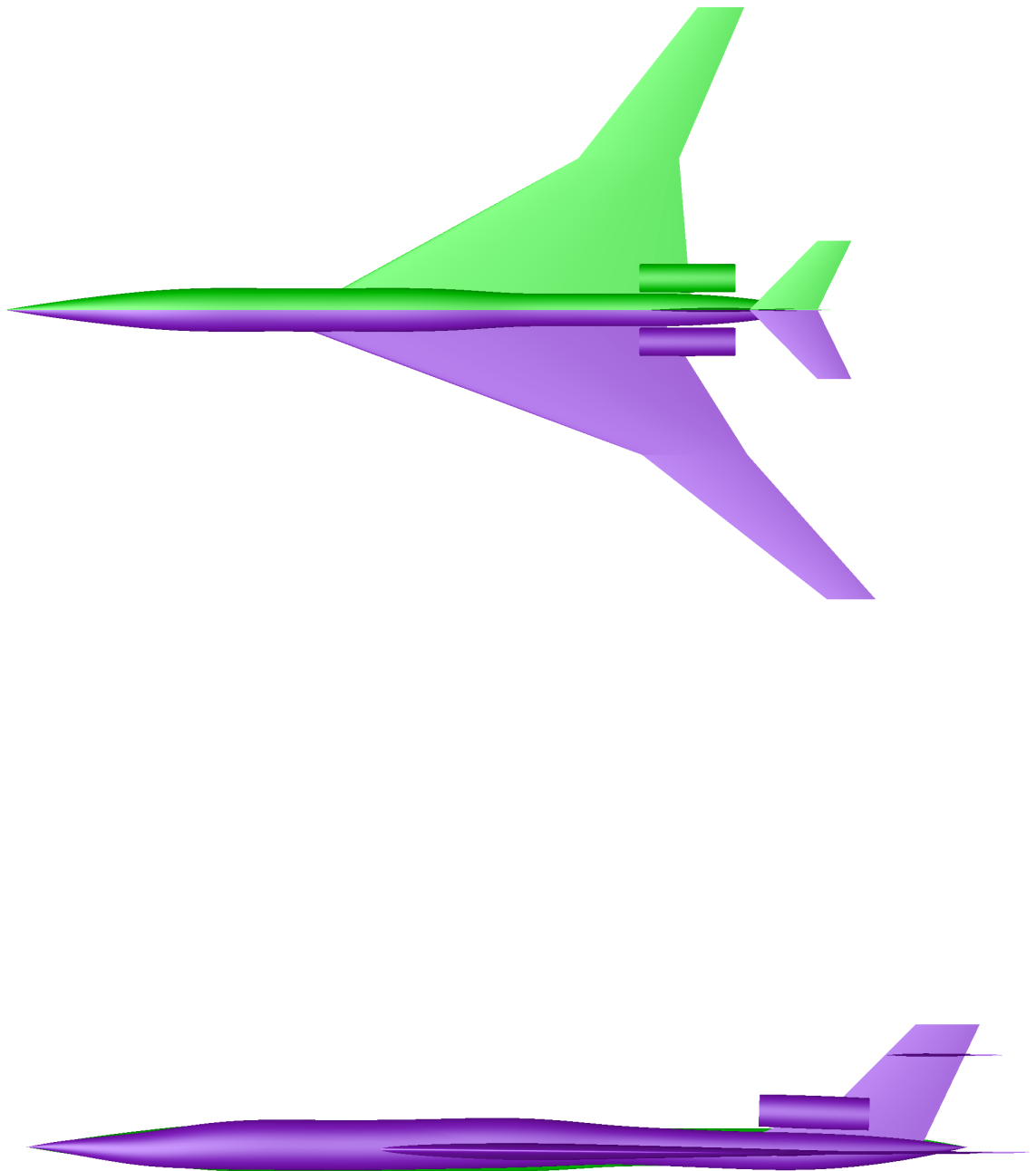Fig. 2    Flowchart of the Various Modules of the QSP107 Design Tool
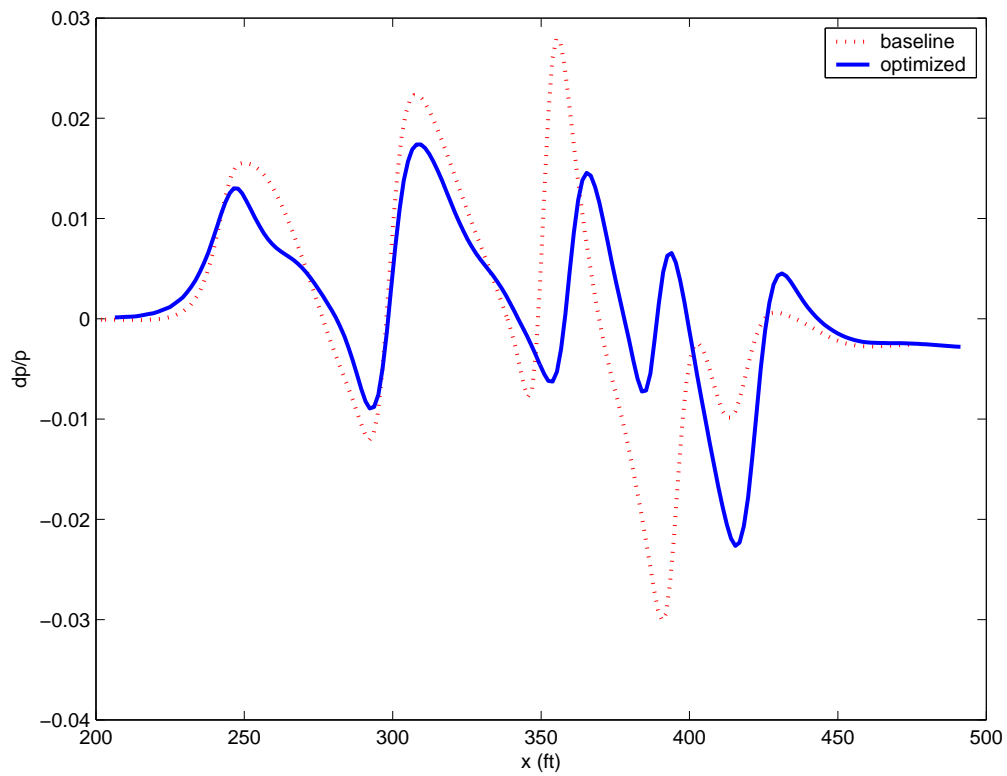
(a) $1^{st}$ Design Iteration



(b) $2^{nd}$ Design Iteration
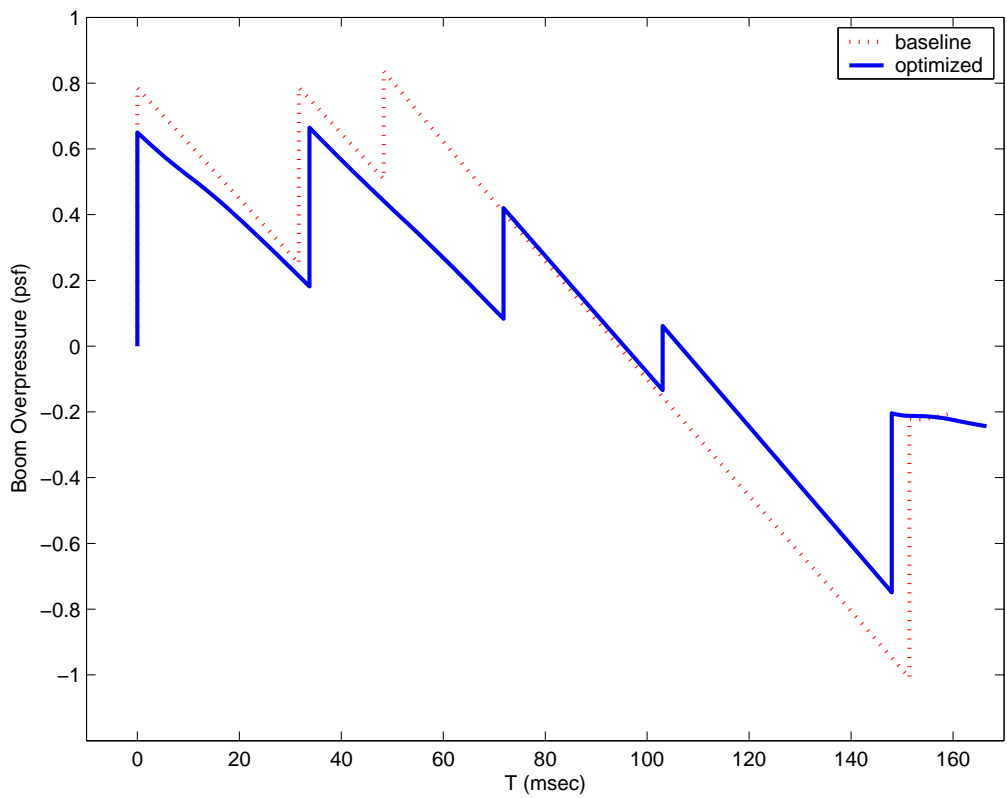
Fig. 3    **Kriging-Based MOGA Results**

(b) Side View (green:baseline, blue:optimized)

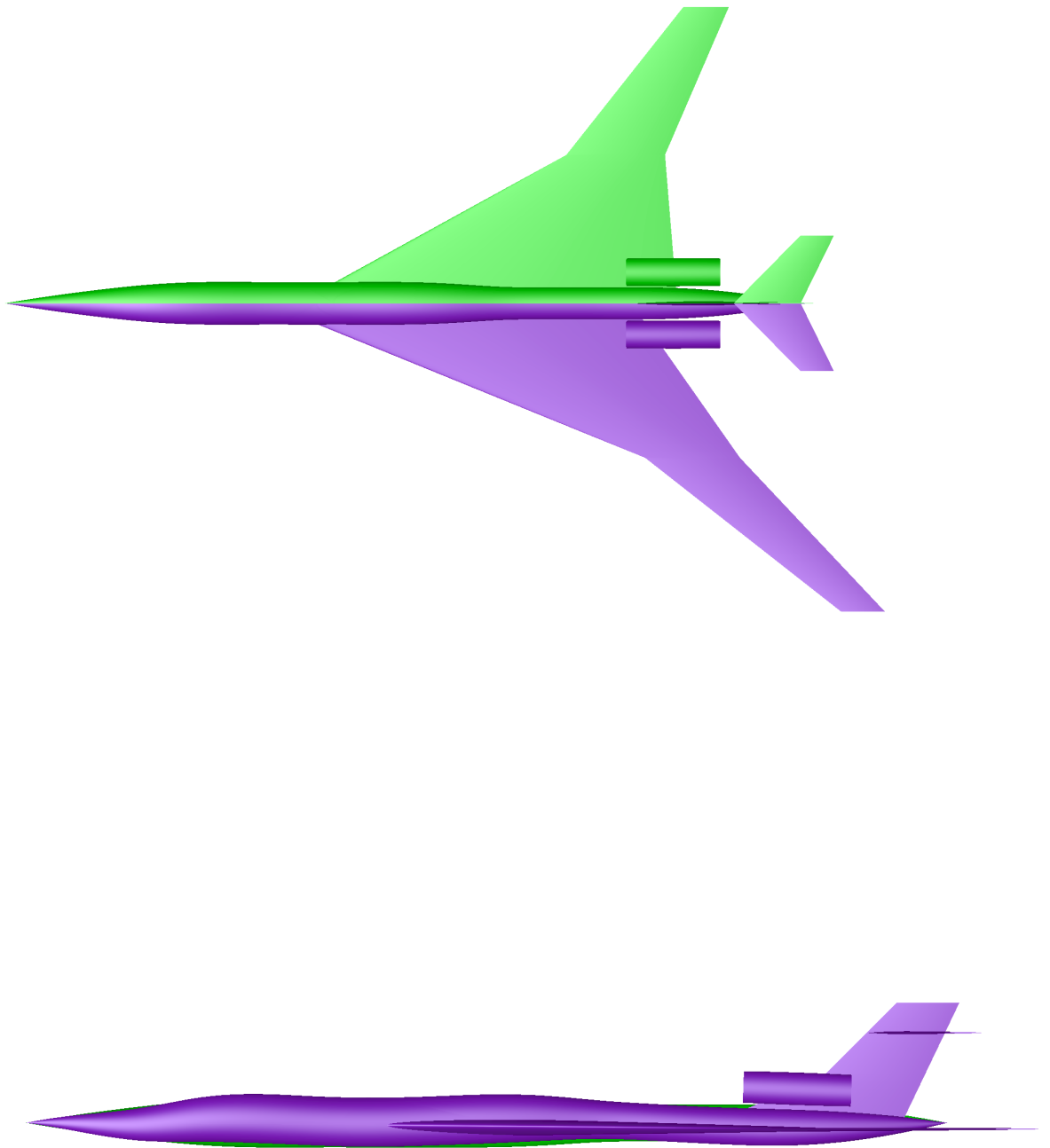**Fig. 4  Configuration of the best $C_D$ design from the Pareto set**

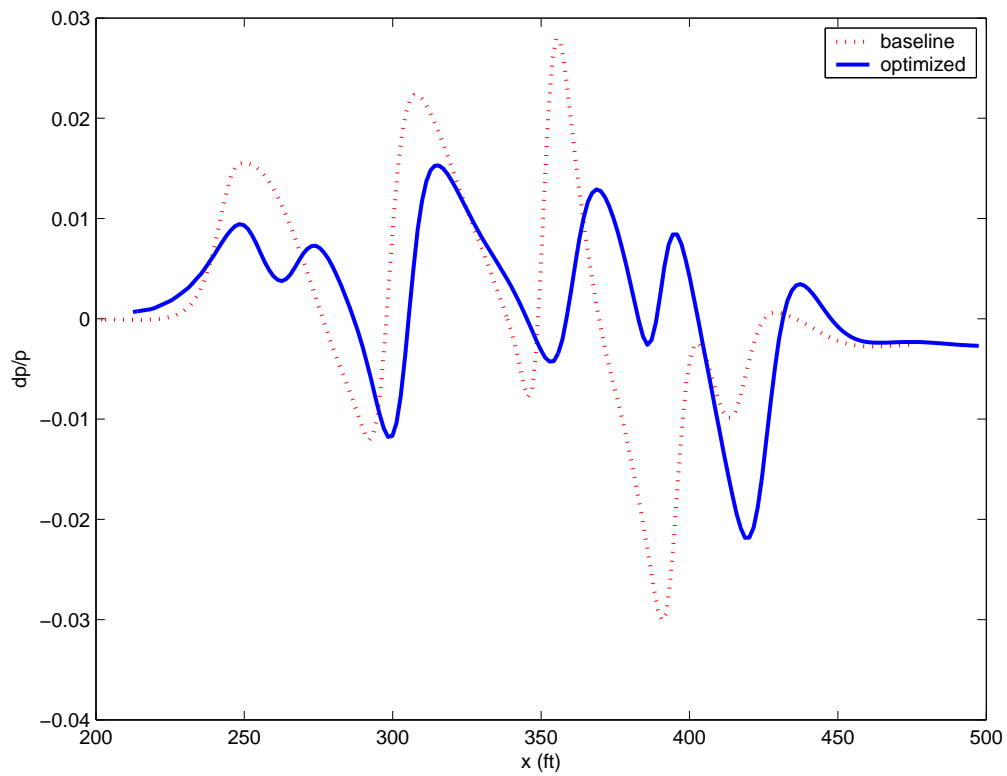(a) Near-field Pressure Distribution



(b) Ground Boom Overpressure

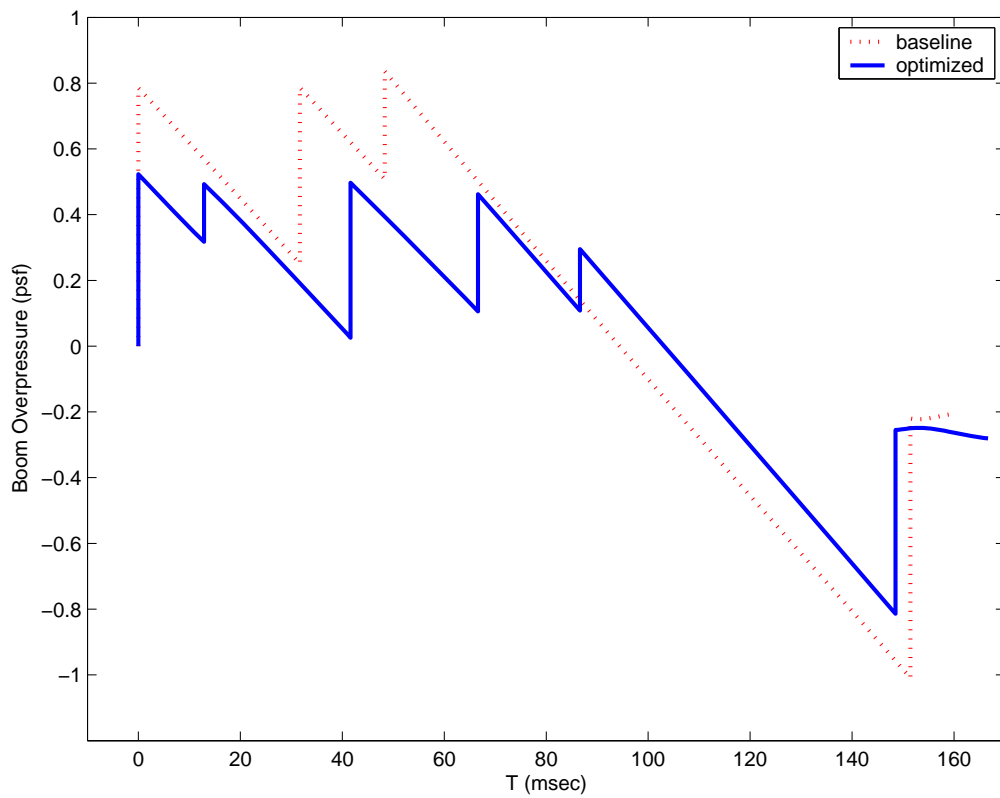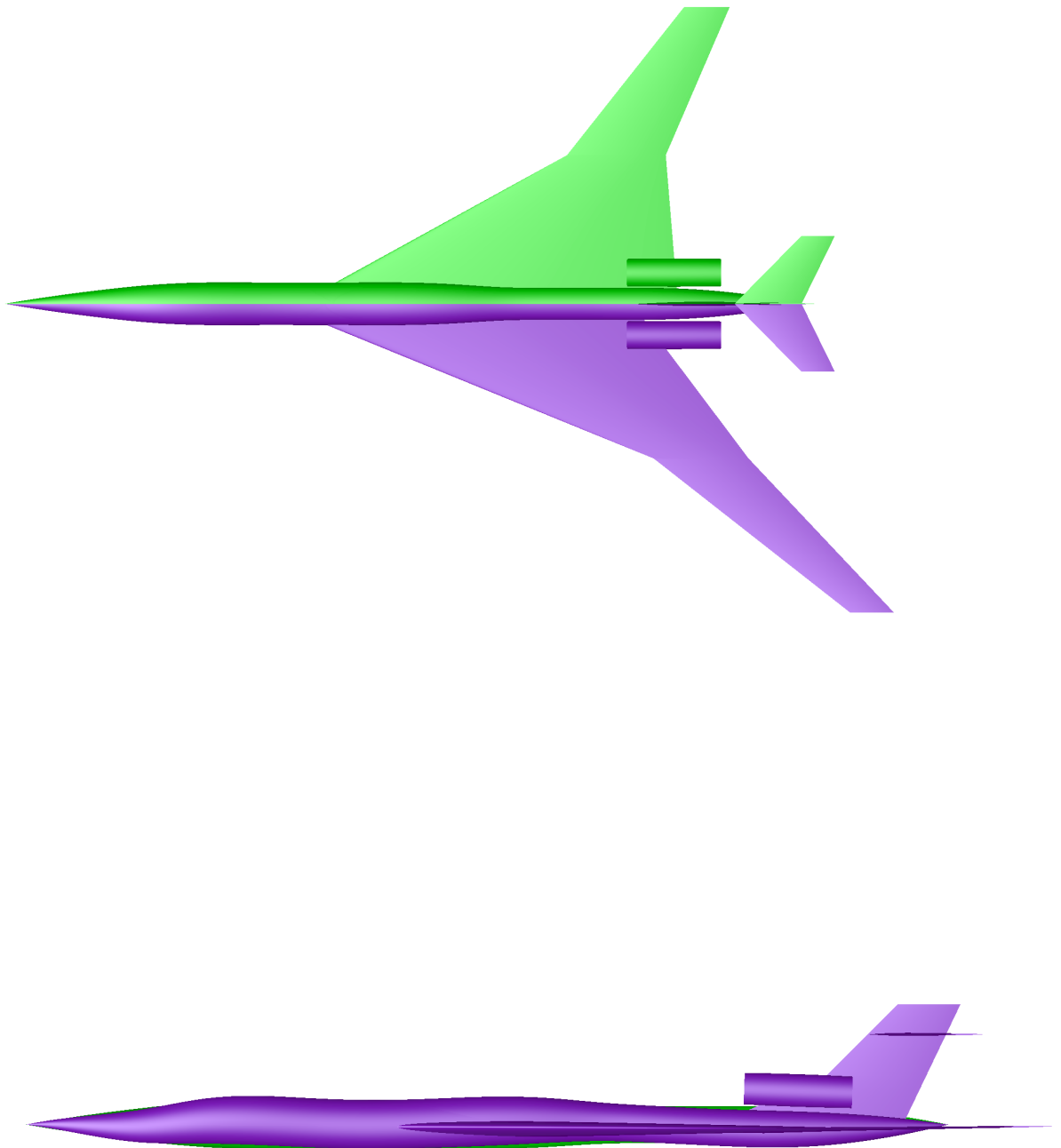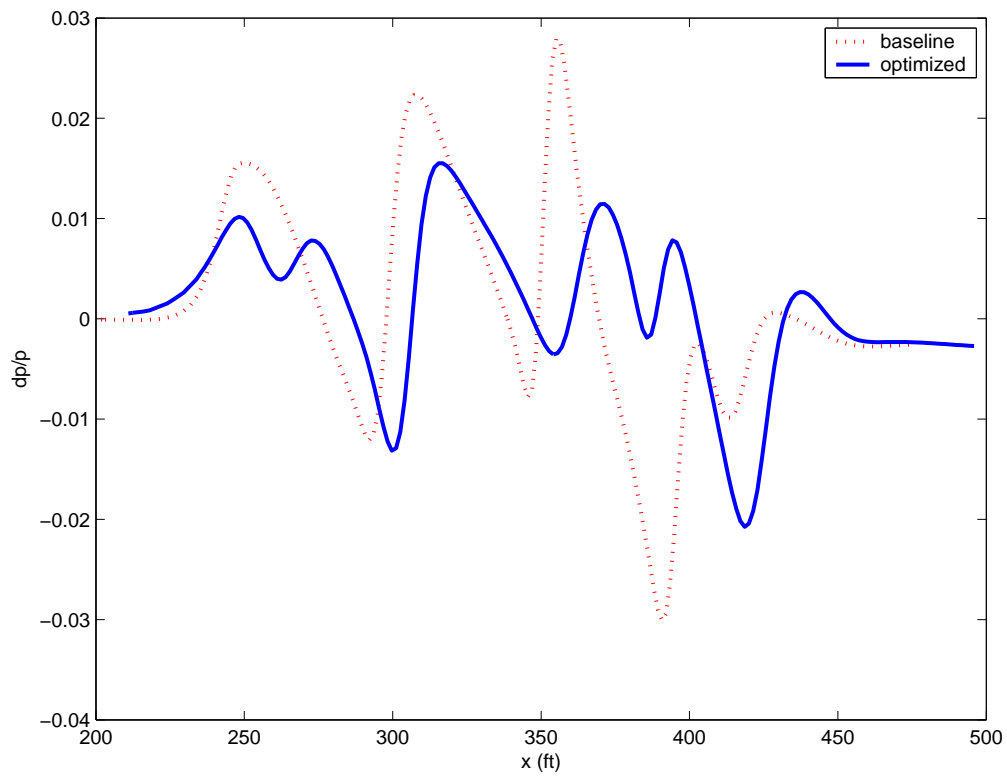Fig. 5    Comparison between baseline and best $C_D$ design

(b) Side View (green:baseline, blue:optimized)

Fig. 6    Configuration of the best boom design from the Pareto set

American Institute of Aeronautics and Astronautics Paper 2004–4325

(a) Near-field Pressure Distribution



(b) Ground Boom Overpressure

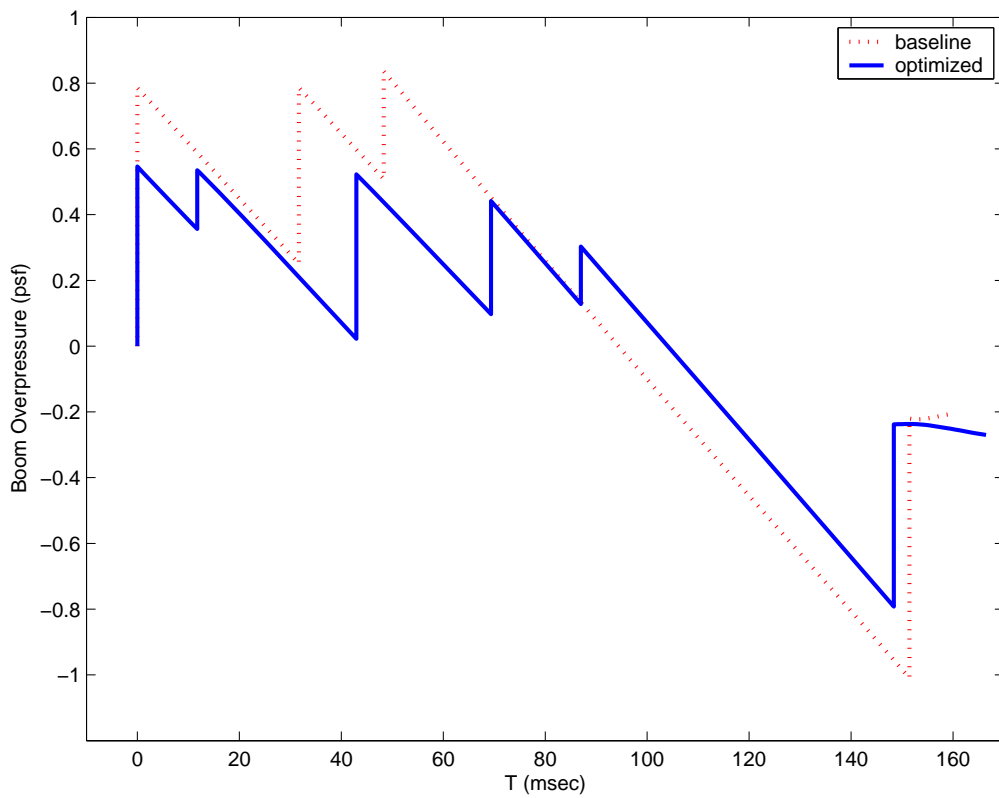**Fig. 7  Comparison between baseline and best boom design**

(b) Side View (green:baseline, blue:optimized)

**Fig. 8   Configuration of one of the best multiobjective designs**
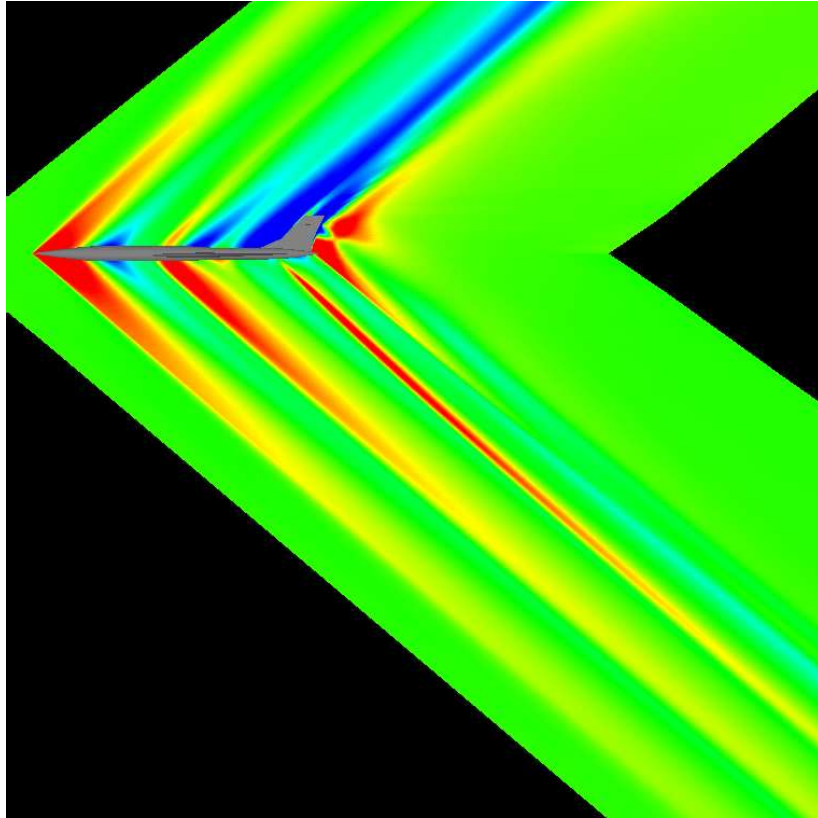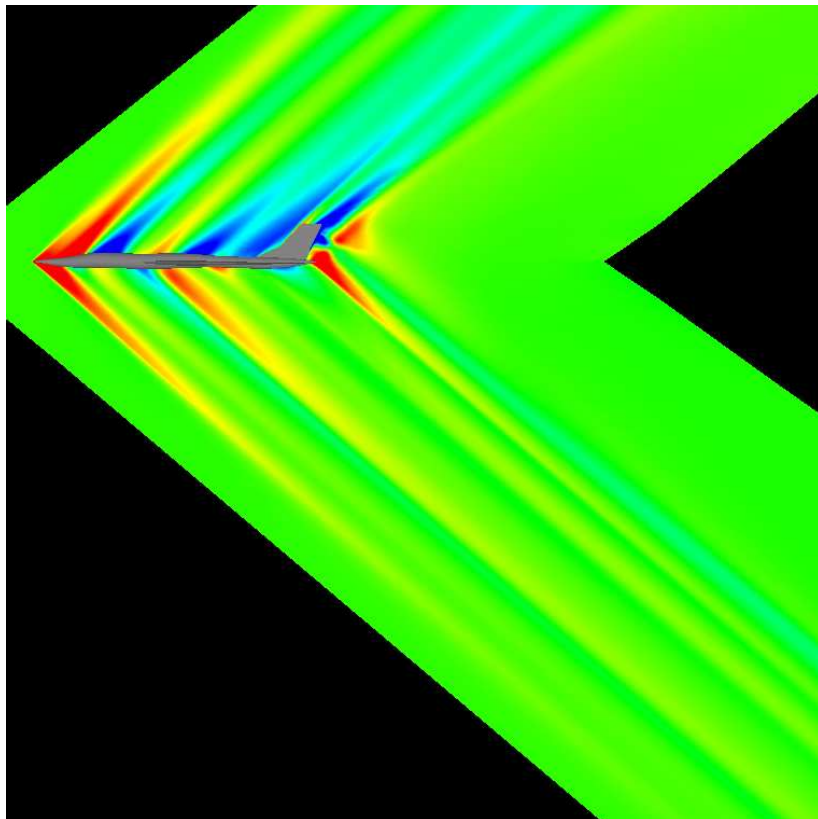
(a) Near-field Pressure Distribution



(b) Ground Boom Overpressure

**Fig. 9   Comparison between baseline and best multiobjective design**

(a) Baseline Design



(b) Best Boom Design

**Fig. 10    Comparison of flow fields between baseline and best boom design**